Joint Centre for Mesoscale Meteorology, Reading, UK

Radar observations of wind-shear splitting within evolving atmospheric Kelvin-Helmholtz billows

K. A. Browning
D. Chapman

Internal Report No. 66

April 1997

Met Office Joint Centre for Mesoscale Meteorology Department of Meteorology
University of Reading PO Box 243 Reading RG6 6BB United Kingdom
Tel: +44 (0)118 931 8425 Fax: +44 (0)118 931 8791
www.metoffice.com

Designed and produced by the Met Office © Crown copyright 2001 01/0240 The Met Office logo is a registered trademark.

Radar observations of wind-shear splitting within evolving atmospheric Kelvin-Helmholtz billows

D. Chapman and K. A. Browning*
Joint Centre for Mesoscale Meteorology

April 16, 1997

Abstract

The high resolution radar at Chilbolton has been used to measure the velocity structure of large-amplitude Kelvin-Helmholtz billows within a precipitating warm frontal zone. A deep layer of frontal shear was observed to split into thin layers of more concentrated shear displaying the characteristic braided structure previously reported within clear-air radar reflectivity patterns and attributed to a splitting of the thermal stratification. The billows were situated within a region of strong wind veer with height and they were orientated at right angles to the mean flow such that air parcels within them were tending to follow helical trajectories up the inclined frontal zone. Radar scans normal to the axes of the billows at different distances from their origin, close to the position of the surface warm front, provided an indication of the evolution of the split shear structure.

*Corresponding author: Joint Centre for Mesoscale Meteorology, Harry Pitt Building, University of Reading, Whiteknights Road, PO Box 240, Reading, Berkshire, RG6 2FN, UK. (The Joint Centre for Mesoscale Meteorology is supported by the Meteorological Office and the Department of Meteorology, University of Reading.)

1 Introduction

Stratified shear instability plays an important role in the atmosphere as Kelvin-Helmholtz billows induce vertical mixing. Whilst many observations of Kelvin-Helmholtz billows have been made using radar, few have shed light on the evolution of billows, or the effect they have on their environment. Those that have (Atlas *et al.*, 1970, Browning and Watkins, 1970) have described the behaviour of the thermal stratification rather than the shear, and it is not obvious that the two should necessarily evolve in the same way. In fact, the distributions of shear obtained by James and Browning (1981) and derived from the study by Takahashi *et al.* (1993) show similar structures to the distribution of thermal stratification implied by clear-air echo studies and this parallel behaviour between the shear and stratification is supported by numerical simulations by Scinocca (1995) who also discussed the outcome of the mixing in 'strong' and 'weak' cases. In this study the structure and evolution of the shear is shown to resemble that expected of the thermal stratification, and the evolution is traced beyond the collapse of the billows.

2 Nature of the data and synoptic context

On the evening of 6 September 1995 a surface warm front approached and passed over southern Britain (see Fig. 1). Between 1500 and 2240 UTC reflectivity and Doppler data were obtained concurrently within an area of light rain and drizzle using the 3 GHz radar at Chilbolton (approximately 80 km north of the Isle of Wight) with a range resolution of 300 m and an unusually high angular resolution of 0.25° (Goddard *et al.*, 1994) . Most of the data were in the form of RHIs (where the radar beam is scanned at different elevations in a fixed bearing (azimuth) - equivalent to a cross section through the atmosphere in a vertical plane passing through the radar) at azimuth spacings of a few degrees. This article is concerned with the dynamical structure and evolution of Kelvin-Helmholtz billows within the strongly sheared frontal zone and it is only the Doppler information from the radar that is used. The location of billows is shown in Fig. 1(b), and the shear responsible for their generation was orientated perpendicular to this cross-section.

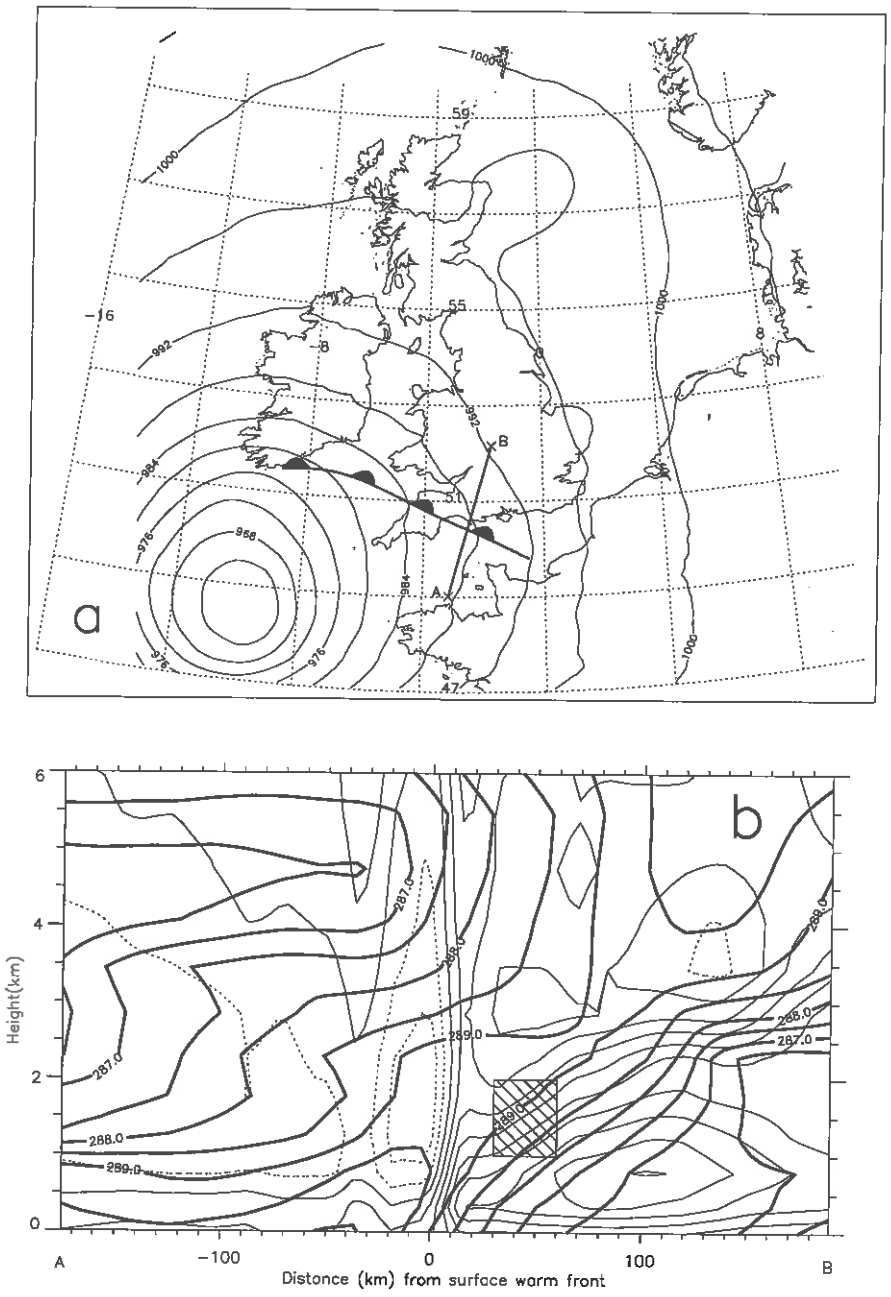

Figure 1: (a) Synoptic chart at 2100 UTC based on a 3 hr forecast from the UKMO Mesoscale Model showing the mean sea level pressure field (mb) and the position of the surface warm front relevant to this study. (b) Vertical cross-section along line AB in (a). Bold contours are of θ_w (K). Lighter contours show the component of wind *into* the plane of this section (intervals of 1 m s^{-1}); solid lines indicate positive values, dotted lines indicate negative values. In the study billows were observed in the region of strong shear between approximately 30 and 60 km north of the surface warm front, as indicated in the figure.

3 Results

Figure 2 shows a schematic plan view of the location of billows (as determined from velocity perturbations in RHIs such as that shown later in Fig. 4(a)) around the radar at times 2100 and 2200 UTC. Vertical cross-sections of Doppler velocity were available in the region of the billows over two periods of time. Between 2010 (which was the time at which billows were first observed) and 2100 UTC observations were made southwest of the radar. From 2200 until 2240 UTC observations were made northeast of the radar. Between 2100 and 2200 UTC observations were made at ranges greater than 50 km, out of the region in which billows occurred.

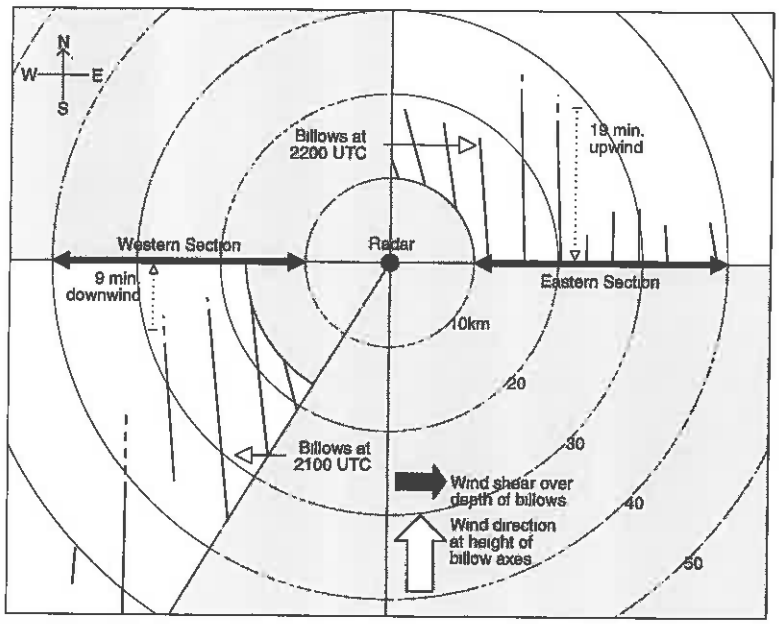

Figure 2: Schematic plan view showing location of billow crests southwest and northeast of Chilbolton Radar at times 2100 and 2200 UTC respectively. No data were available in the shaded region. Locations of vertical sections described in text and in Fig. 4 are shown as bold arrows labelled Western Section and Eastern Section respectively. Broad arrows at foot of diagram show that there was a strong wind component along the billow axes, at right angles to the main component of shear. Thus the billows went through their life cycle from south to north; the dotted arrows show times of the western and eastern section in relation to the northern (decaying) ends of the billows.

The billows had a wavelength of around 5 km when observed to the west of the radar, and around 4 km to the east. Other properties such as amplitude and phase speed of the billows were also found to be very similar on both sides of the radar, and billows to the west of the radar are thought to have behaved in a broadly similar way to those to the east.

The surface warm front (as defined by sharp gradients in the wind field from radar observations) was moving northwards at approximately 10 m s^{-1}. The patch of billows also appeared to have a northwards component of velocity approximately equal to this (although this could not be determined accurately), implying that the region containing billows was fixed relative to the surface front. A hodograph derived from radar data at 2210 UTC *within* the billows to the northeast of the radar is shown in Fig. 3. This shows a layer of shear between 0.4 and 1.6 km in height within which there existed a strong west-east component of shear perpendicular to the billow axes. At the mean height of the billows, the hodograph shows a southerly component of wind around 20 m s^{-1}, so in a reference frame fixed relative to the front, there was a southerly wind of around 10 m s^{-1} relative to the billow patch. As the billows developed at the southern end of the patch (presumably due to large scale forcing in this region), they were advected northwards whilst continuing to grow; then they broke and decayed at the northern end of the patch. Thus successive west-east RHIs intersected the billows at different stages in their evolution as the patch moved northwards over a west-east line through the radar. The along-axis length of the billows appeared to be of the order of 30 km, which gives a lifespan of each billow of the order of 50 minutes (although the patch of billows existed for over 3 hours because of the continuous regeneration of the billows at their southern end).

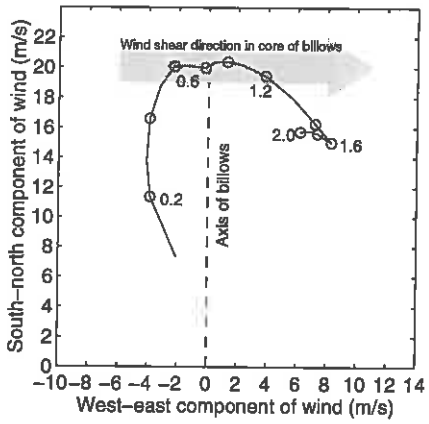

Figure 3: Hodograph showing wind velocity as a function of height within billows north east of radar at 2210 UTC. Height labels in kilometres; values plotted at 0.2 km intervals.

Figures 4(c)-(f) show cross-sections of the vertical shear of the westerly component of the horizontal wind, derived from Doppler RHIs in a west-east direction such as that shown in Fig. 4(a). Figures 4(a)-(d) show the active parts of the billows to the east of the radar, and Figs. 4(e) and (f) show the shear downwind of the billows to the west of the radar. Also shown in Fig. 4(a) is a mass-streamfunction derived by integrating the continuity equation upwards from the ground. The streamfunction

is superimposed on the Doppler winds, indicating parcel trajectories projected onto the plane of the RHI (there was a mean southerly wind of 20 m s^{-1} into this plane at the level of the billows). This shows that air parcels within the billows (centred at a height of approximately 1 km) followed trajectories that were approximately helical, with the main axis aligned in a south-north direction. The main assumption in deriving this streamfunction was that there was no variation of the south-north component of velocity along the length of the billows. There is clearly a strong correlation between the rolls shown by the streamfunction and the undulations in the Doppler data, indicating that the assumption was valid and that the billows were essentially 2-dimensional in the region of the RHI. The same was true of a west-east RHI obtained at 2210 UTC (not shown). However, a similar manipulation of the Doppler data to give the streamfunction at 2200 UTC (also not shown) showed a poor correlation, indicating that at that time the air motion was 3-dimensional in the region of the RHI.

Figure 4(b) shows the vertical velocity (with the streamfunction from Fig. 4(a) superimposed) which was obtained from the Doppler velocity with the same 2-dimensional assumption that was used to derive the streamfunction. It can be seen that the billows induced vertical velocities as large as $\pm$ 3 m s^{-1}.

Parts of the cross-sections of shear shown in Figs. 4(c)-(f) and a cross-section derived from the RHI at 2210 UTC were averaged (over approximately. 14 to 24 km east of the radar in Figs. 4(c) and (d), and 20 to 30 km west in Figs. 4(e) and (f)) to generate the mean shear profiles shown in Figs. 5(a) and (b). The approximate location of the cross-section relative to the end of the billows that were averaged over was determined, and knowledge of the mean wind through the billows allowed the time of each profile within the lifecycle of the billows to be calculated. These varied from 19 to 25 minutes upwind of the region of collapse in Fig. 5(a) and from 9 to 19 minutes downwind of the region of collapse in Fig. 5(b).

4 Discussion

The sequence of shear profiles (Figs. 5(a) and (b)) shows that within the billows (Fig. 5(a)), a single shear layer became split into two over a short period of time. Downwind of the billows (Fig. 5(b)) there existed a broad split shear layer (solid line), though further downwind the split was less well defined (dotted line). The greater depth of the shear layer to the west of the radar (Fig. 5(b)) than to the

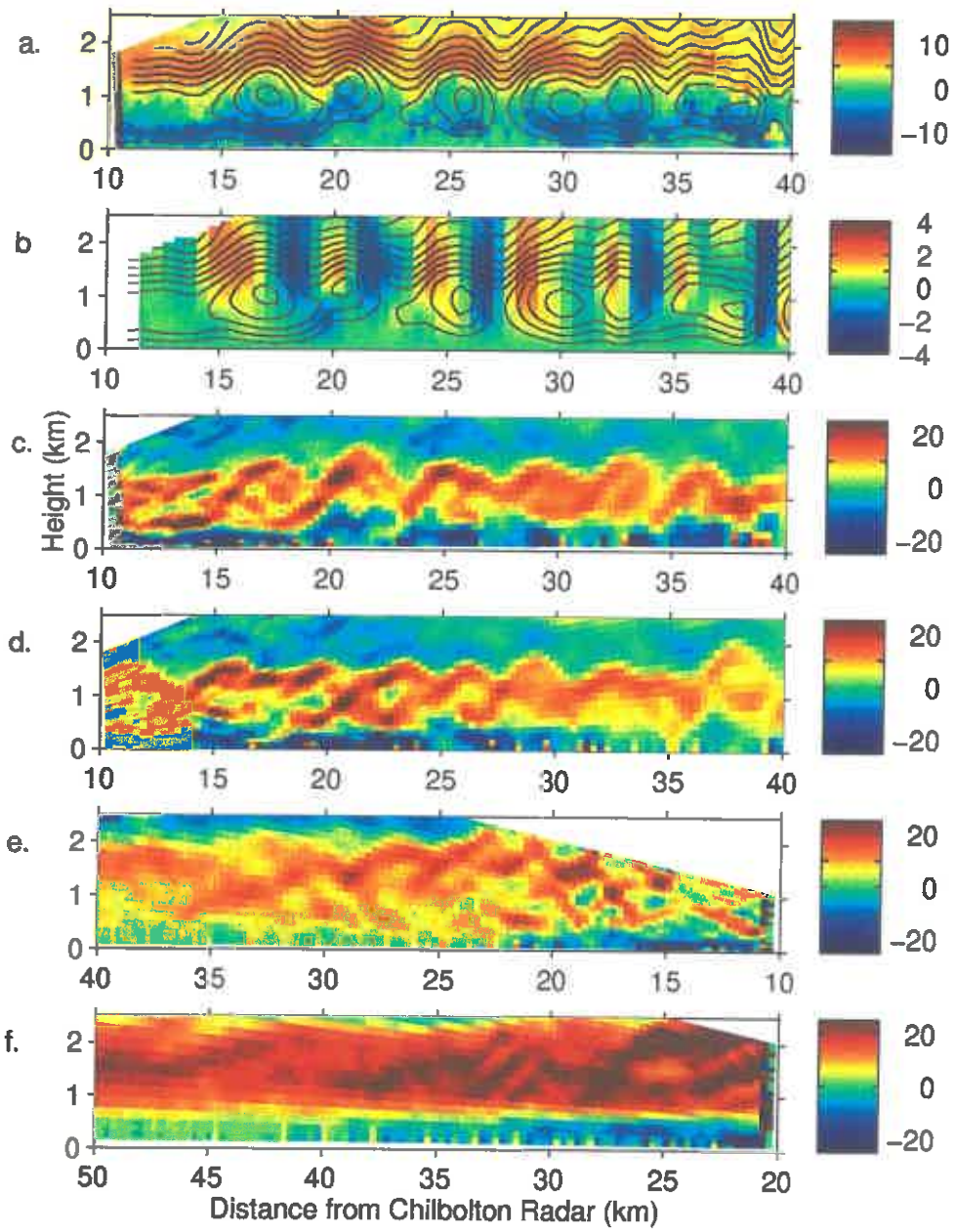

Figure 4: (a) Vertical west-east cross section (RHI) of Doppler velocity, effectively giving westerly wind components (m s^{-1}, blue to the left and red toward the right) at 2220 UTC. Superimposed are contours of a mass-streamfunction (intervals of 1000 kg m^{-1} s^{-1}) projected onto the plane of the RHI. (b) As (a), except shading shows vertical velocity (m s^{-1}) at 2220 UTC. (c)-(f) Vertical west-east cross-sections of shear (m s^{-1} km^{-1}) derived from Doppler velocity RHIs at times 2220, 2200, 2100 and 2020 UTC respectively. (a)-(d) are eastern sections obtained upwind, and (e) and (f) are western sections obtained downwind of the region of billow collapse.

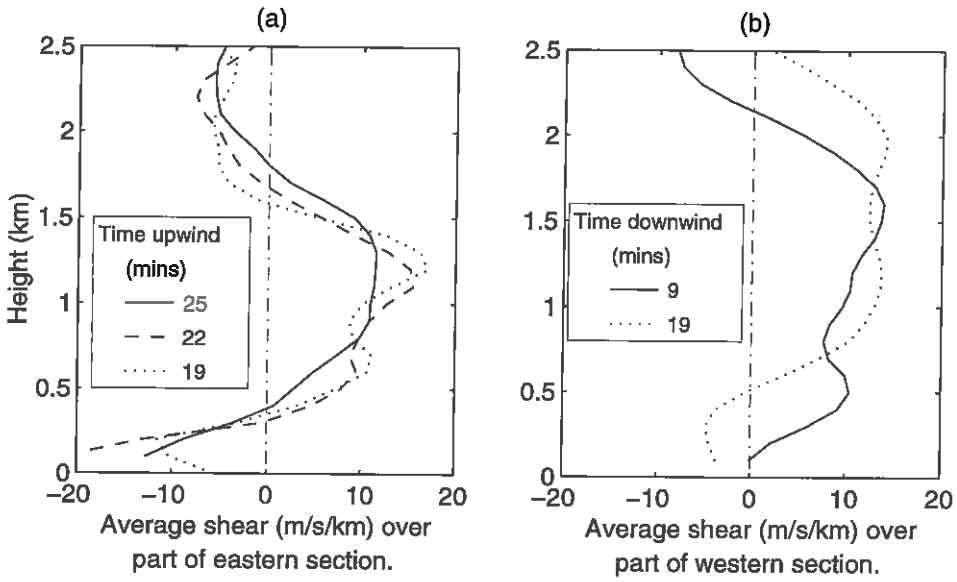

Figure 5: Profiles of shear (m s^{-1} km^{-1}) averaged horizontally approximately (a) 25, 22 and 19 minutes upwind and (b) 9 and 19 minutes downwind of the collapse of the billows. These profiles are derived from averages of shear cross-sections at times 2220, 2210, 2200, 2100 and 2020 UTC, respectively.

east (Fig. 5(a)) is probably due to an imposed larger-scale variability in the depth of frontal shear. The detailed evolution of the structure of the shear layer can be observed in the relevant parts of Figs. 4(c)-(f).

Many observations of Kelvin-Helmholtz billows in the atmosphere have been made previously using radar to detect clear-air echoes from regions of high refractive index variance occurring at airmass boundaries (Atlas *et al.*, 1970, Browning and Watkins, 1970, Browning, 1971, Hardy *et al.*, 1973) . For a comprehensive review see Gossard (1990). The distributions of reflectivity (and thus by implication the thermal stratification) obtained in this manner through billows are qualitatively similar to the distribution of shear shown in Figs. 4(c) and (d), indicating that in this case momentum was effectively mixed in the same way as the stratification, at least to a first approximation.

The evolution of the shear layer in this case also resembles the evolution of the thermal stratification within billows of similar dimensions deduced from clear-air radar data by Browning and Watkins (1970). However, a difference is that they observed the stratification to become split into two long-lived layers downwind of the billows whereas the split shear was short-lived in the present case. The proximity of the frontal zone to the ground makes our case significantly different. It is likely that the strong south-north component of shear due to the boundary layer (Fig. 3) prevented a long-lived

split from being sustained within the frontal zone. In view of the proximity of the boundary layer it is perhaps surprising that such well-formed billows were able to develop at all. Despite the south-north component of shear penetrating into the lower parts of the billows themselves, they had a lifespan of around 50 minutes, compared to a lifespan of around 15 minutes found by Browning and Watkins when there was no such potentially disruptive shear at the boundaries of the billows.

Numerical models (Scinocca, 1995, Sykes and Lewellen, 1982, Klaasen and Peltier, 1981) and laboratory observations (Thorpe, 1985) of Kelvin-Helmholtz billows have shown that their breakdown (under idealised conditions) is caused by convective instability forming vortices orientated perpendicular to the billows. Whilst the billows are still growing this instability is suppressed and they remain essentially 2-dimensional. Once the billows have reached their maximum amplitude the convective instability is allowed to grow, and the billows start to attain a 3-dimensional structure. The previously noted failure of the streamfunction calculation for the RHI at 2200 UTC (corresponding to the section within the billows closest to their northern end) may to be due to the onset of this 3-dimensional structure, or it may be due to the onset of less organised 3-dimensional turbulence as the convectively unstable regions cause the wave to 'break'.

Kelvin-Helmholtz billows have been shown to be an important cause of clear-air turbulence (CAT) (Browning *et al.*, 1970) , so at any altitude Kelvin-Helmholtz billows as strong as these could constitute an aviation hazard. However, in cases such as this the hazard is greatly increased due to the concentration of the moderate mean shear into regions of strong shear (up to around 25 m s^{-1} km^{-1} in this case) extending down to a few hundred metres above the ground. This would be most relevant during aircraft take-off and landing when the localised effects of the billows could lead to substantial under-estimation of the low-altitude wind shear, even at airports where wind-profilers were in use.

5 Acknowledgements

We are grateful to Drs. Anthony Illingworth and Mark Blackman for their part in the data acquisition, and thank the Radio Communications Research Unit at Rutherford Appleton Laboratory for access to the Chilbolton radar. We are also grateful to Peter Panagi for supplying the Mesoscale Model data. Daniel Chapman is supported by a studentship from the Natural Environment Research Council.

References

Atlas, D., Metcalf, J. I., Richter, J. H., and Gossard, E. E. (1970). The birth of CAT and microscale turbulence. *J. Atmos. Sci.*; **27**, 903–913.

Browning, K. A. (1971). Structure of the atmosphere in the vivinity of large-amplitude Kelvin-Helmholtz billows. *Q. J. R. Meteorol. Soc.*; **97**, 283–299.

Browning, K. A. and Watkins, C. D. (1970). Observations of clear-air turbulence by high power radar. *Nature*; **227**, 260–263.

Browning, K. A., Watkins, C. D., Starr, J. R., and McPherson, A. (1970). Simultaneous measurements of clear-air turbulence at the tropopause by high-power radar. *Nature*; **228**, 1065–1067.

Goddard, J. W. F., Eastment, J. D., and Thurai, M. (1994). The Chilbolton advanced meteorological radar: a tool for multidisciplinary research. *Electronics and Communications Engineering Journal*; **6**, 77–86.

Gossard (1990). Radar research on the Atmospheric Boundary Layer. Chapter 27a in *Radar in Meteorology*. Ed. D. Atlas. American Meteorological Society, pages 477–527.

Hardy, K. R., Reed, R. J., and Mather, G. K. (1973). Observation of Kelvin Helmholtz billows and their meso-scale environment by radar, instrumented aircraft and a dense radiosonde network. *Q. J. R. Meteorol. Soc.*; **99**, 279–293.

James, P. K. and Browning, K. A. (1981). An observational study of primary and secondary billows in the free atmosphere. *Q. J. R. Meteorol. Soc.*; **107**, 351–365.

Klaasen, G. P. and Peltier, W. R. (1981). The onset of turbulence in finite-amplitude Kelvin-Helnholtz billows. *J. Fluid Mech.*; **155**, 1–35.

Scinocca, G. P. (1995). The mixing of mass and momentum by Kelvin-Helmholtz billows. *J. Atmos. Sci.*; **52**, 2509–2530.

Sykes, R. I. and Lewellen, W. S. (1982). A numerical study of breaking Kelvin-Helmholtz billows using a Reynolds-stress turbulence closure model. *J. Atmos. Sci.*; **39**, 1506–1520.

Takahashi, N., Uyeda, H., and Kikuchi, K. (1993). A Doppler radar observation on wave-like echoes generated in a strong vertical shear. *J. Meteorol. Soc. Japan*; **71**, 357–365.

Thorpe, S. A. (1985). Laboratory observations of secondary structures in Kelvin-Helmholtz billows and consequences for ocean mixing. *Geophys. Astrophys. Fluid Dyn.*; **34**, 175–199.

CURRENT JCMM INTERNAL REPORTS

This series of JCMM Internal Reports, initiated in 1993, contains unpublished reports and also versions of articles submitted for publication. The complete set of Internal Reports is available from the National Meteorological Library on loan, if required.

1. **Research Strategy and Programme.**
   K A Browning et al
   January 1993

2. **The GEWEX Cloud System Study (GCSS).**
   GEWEX Cloud System Science Team
   January 1993

3. **Evolution of a mesoscale upper troposheric vorticity maximum and comma cloud from a cloud-free two dimensional potential vorticity anomaly.**
   K A Browning
   January 1993

4. **The Global Energy and Water Cycle**
   K A Browning
   July 1993

5. **Structure of a midlatitude cyclone before occlusion.**
   K A Browning and N Roberts
   July 1993

6. **Development in Systems and Tools for Weather Forecasting**
   K A Browning and G Szejwach
   July 1993

7. **Diagnostic study of a narrow cold frontal rainband and severe winds associated with a stratospheric intrusion.**
   K A Browning and R Reynolds
   August 1993

8. **Survey of perceived priority issues in the parametrizations of cloud-related processes GCMs.**
   K A Browning
   September 1993

9. **The Effect of Rain on Longwave Radiation.**
   I Dharssi
   September 1993

10. **Cloud Microphysical Processes - A Description of the Parametrization used in the Large Eddy Model.**
    H Swann
    July 1994

11. **An Appreciation of the Meteorological Research of Ernst Kleinschmidt.**
    A J Thorpe
    May 1992

12. **Potential Vorticity of Flow Along the Alps.**
    A J Thorpe, H Volkert and Dietrich Heimann
    August 1992

13. **The Representation of Fronts.**
    A J Thorpe
    January 1993

14. **A Parametrization Scheme for symmetric Instability: Test for an Idealised Flow.**
    C S Chan and A J Thorpe
    February 1993

15. **The Fronts 92 Experiment: a Quicklook Atlas**
    Edited by T K Hewson
    November 1993

16. **Frontal wave stability during moist deformation frontogenesis.**
    Part 1. Linear wave dynamics
    C H Bishop and A J Thorpe
    May 1993

17. **Frontal wave stability during moist deformation frontogenesis.**
    Part 2. The suppression of non-linear wave development.
    C H Bishop and A J Thorpe
    May 1993

18. **Gravity waves in sheared ducts.**
    C H Bishop and A J Thorpe
    October 1993

19. **Potential Vorticity and the Electrostatics Analogy: Quasi-Geostrophic Theory.**
    C Bishop and A J Thorpe
    November 1993

20. **Recent Advances in the Measurement of Precipitation by Radar.**
    A J Illingworth - April 1993

21. **Micro-Physique et Givrage. Cloud Microphysics and Aircraft Icing.**
A J Illingworth
May 1993

22. **Differential Phase Measurements of Precipitaiton.**
M Blackman and A J Illingworth
May 1993

23. **Estimation of Effective Radius of Cloud Particles from the Radar Reflectivity.**
N I Fox and A J Illingworth
May 1993

24. **A Simple Method of Dopplerising a Pulsed Magnetron Radar.**
L Hau, A J Illingworth and J Eastment
November 1993

25. **Radiation and Polar Lows.**
George C Craid
February 1994

26. **Collected preprints submitted International Symposium on the Life Cycles of Ectratropical Cyclones; Bergen, Norway, 27 June - 1 July 1994**
April 1994

27. **Convective Frontogenesis**
Douglas J Parker and Alan J Thorpe
April 1994

28. **Improved Measurement of the Ice Water Content in Cirrus Using a Total Water Evaporator.**
Philip R A Brown and Peter N Francis
April 1994

29. **Mesoscale Effects of Dry Intrusion within a vigorous Cyclone**
K A Browning and B W Golding
April 1994

30. **GEWEX Cloud System Study, Science Plan**
May 1994

31. **Parametrization of Momentum Transport by Convectively Generated Gravity Waves**
R Kershaw
February 1995

32. **Mesoscale Modelling Newsletter, No.5 -**
May 1994

33. **Observations of the mesoscale sub-structure in the cold air of a developing frontal cyclone.**
K A Browning, S A Clough, C S A Davitt, N M Roberts and T D Hewson
May 1994

34. **Longwave Radiative Forcing of a Simulated Tropical Squall Line**
Imtiaz Dharssi
July 1994

35. **On the nature of the convective circulation at a Kata-cold front**
K A Browning
September 1994

36. **Collective preprints of papers submitted to the COST-75 International Seminar on Advanced Weather Radar Systems, Brussels, 20-23 September 1994**
November 1994

37. **Use of satellite imagery to diagnose events leading to frontal thunderstorms: Parts 1 and 11 of a case study.**
K A Browning and N M Roberts
November 1994

38. **The role of spaceborne millimeter-wave radar in the global monitoring of ice cloud.**
P R A Brown, A J Illingworth, A J Heymsfield, G M McFarquahar, K A Browning and M Gosset.
December 1994

39. **Potential Vorticity Inversion**
Michal Ziemianski
October 1994

40. **Theory of mature tropical cyclones; A comparison between Kleinschmidt (1951) and Emanual (1986)**
Suzanne L Gray
December 1994

41. **Dispersion and removal of pollutants during the passage of an atmospheric frontal system**
N R Gimson
December 1994

42. **The role of snow sublimation in frontogenesis**
D J Parker and A J Thorpe
December 1994

43. **Potential vorticity and the electrostatics Analogy: Ertel-Rossby formulation**
A J Thorpe and C H Bishop.
December 1994

44. **Mesoscale aspects of extratropical cyclones: and observational perspective**
K A Browning
January 1995

46. **Generation of near-surface gusts by deep convection**
K Nakamura and R Kershaw
April 1995

47. **Attribution concepts applied to the omega equation**
S A Clough, C S A Davitt and A J Thorpe
June 1995

48. **Parametrization of mixed-phase cloud and precipitation**
Susan P Ballard and M Gerard Hutchinson
June 1995

49. **Short-range forecasting of stratocumulus: Initialization V Prediction**
Susan P Ballard, Simon D Jackson and B Macpherson
June 1995

50. **Contributions of the JCMM/Dept of Meteorology Radar Group to the 27th AMS Radar Meteorology Conference, Vail October 1995.**
June 1995

51. **Cold pools in shear**
Douglas J Parker
September 1995

52. **High-resolution analysis of frontal fracture**
K A Browning, S P Ballard and C S A Davitt
September 1995

53. **The Albedo of Broken Cloud Fields: Calculations using a modified two stream radiation code.**
Imatiaz Dharssi and Roy Kershaw
October 1995

54. **Parametrization of momentum transport by convection. I: Theory and cloud modelling results.**
P Kershaw and D Gregory
November 1995

55. **Variation of frontal structure along a cold front**
K A Browning and N M Roberts
November 1995

56. **Secondary Frontal Waves**
Douglas Parker
December 1995

57. **Objective Fronts**
T D Hewson
March 1996

58. **Mesoscale analysis of the activation of a cold front during cyclogenesis**
K A Browning, N M Roberts and A J Illingworth
June 1996

59. **Investigation of different representations of rain in a 1-d evaporation model**
H Swann
May 1996

60. **Parametrization of diabatic processes in the inversion of the omega-equation**
M Athanassiadou and A J Thorpe

61. **The role of the environmental flow in the development of secondary frontal cyclones**
I A Renfrew, A J Thorpe and C H Bishop

62. **Consequences of the geostrophic momentum approximation on barotropic instability**
S Malardel, A J Thorpe and A Joly
June 1996

63. **Contributions to the AMS/RMS Conference on Mesoscale Processes Reading,** 9 - 13 September 1996
June 1996

64. **Vorticity and Potential Vorticity Stratified Flows Interacting with an Isolated Obstacle.**
Jorge A Gutierrez and A J Thorpe - September 1996

65. **Triple Point Development: Two Case Studies**
Douglas Parker
September 1996

66. **Radar observations of wind-shear splitting within evolving atmospheric Kelvin-Helmholtz billows**
D. Chapman and K.A. Browning
April 1997

Met Office Joint Centre for Mesoscale Meteorology Department of Meteorology
University of Reading PO Box 243 Reading RG6 6BB United Kingdom
Tel: +44 (0)118 931 8425 Fax: +44 (0)118 931 8791
www.metoffice.com